0026-895X/11/7901-24–33$20.00
MOLECULAR PHARMACOLOGY
Copyright © 2011 The American Society for Pharmacology and Experimental Therapeutics
Mol Pharmacol 79:24–33, 2011

Vol. 79, No. 1
68155/3648724
Printed in U.S.A.

Rational Design of a Selective Covalent Modifier of G Protein $\beta\gamma$ Subunits

Axel L. Dessal, Roger Prades, Ernest Giralt, and Alan V. Smrcka

Department of Pharmacology and Physiology, University of Rochester, School of Medicine and Dentistry, Rochester, New York (A.L.D., A.V.S.); Institute for Research in Biomedicine, Barcelona Science Park, Barcelona, Spain (R.P., E.G.); and Department of Organic Chemistry, University of Barcelona, Barcelona, Spain (E.G.)

Received August 12, 2010; accepted September 29, 2010

ABSTRACT

G protein-coupled receptors transduce signals through heterotrimeric G protein Gα and G$\beta\gamma$ subunits, both of which interact with downstream effectors to regulate cell function. G$\beta\gamma$ signaling has been implicated in the pathophysiology of several diseases, suggesting that G$\beta\gamma$ could be an important pharmaceutical target. Previously, we used a combination of virtual and manual screening to find small molecules that bind to a protein-protein interaction "hot spot" on G$\beta\gamma$ and block regulation of physiological effectors. One of the most potent and effective compounds from this screen was selenocystamine. In this study, we investigated the mechanism of action of selenocystamine and found that selenocysteamine forms a covalent complex with G$\beta\gamma$ by a reversible redox mechanism. Mass spectrometry and site-directed mutagenesis suggest that selenocysteamine preferentially modifies GβCys204, but also a second undefined site. The high potency of selenocystamine in G$\beta\gamma$ inhibition seems to arise from both high reactivity of the diselenide group and binding to a specific site on Gβ. Using structural information about the "hot spot," we developed a strategy to selectively target redox reversible compounds to a specific site on G$\beta\gamma$ using peptide carriers such as SIGCAFKILGY(-cysteamine) [SIGC(-cysteamine)]. Mass spectrometry and site-directed mutagenesis indicate that SIGC(-cysteamine) specifically and efficiently leads to cysteamine (half-cystamine) modification of a single site on Gβ, likely GβCys204, and inhibits G$\beta\gamma$ more than a hundred times more potently than cystamine. These data support the concept that covalent modifiers can be specifically targeted to the G$\beta\gamma$ "hot spot" through rational incorporation into molecules that noncovalently bind to G$\beta\gamma$.

Introduction

G protein $\beta\gamma$ (G$\beta\gamma$) subunits, when activated by GPCRs, interact with many target proteins, including phospholipase C β2 (PLCβ2), PLCβ3, phosphoinositide 3-kinase γ, G protein-coupled receptor kinase 2 (GRK2), adenylyl cyclases, N-type calcium channels, and G protein-activated inwardly rectifying potassium channels (Gilman, 1987; Oldham and Hamm, 2006; Smrcka, 2008; Dupré et al., 2009). Through these interactions, G$\beta\gamma$ regulates many physiological processes, such as neutrophil chemotaxis, vascular cell proliferation, and cardiac chronotropy. Because overactivation of G$\beta\gamma$ signaling has been implicated in the pathophysiology of conditions such as cancer (Bookout et al., 2003; Daaka, 2004), heart failure (Koch et al., 1995; Rockman et al., 2002), and chronic inflammation (Hirsch et al., 2000; Li et al., 2000), G$\beta\gamma$ may be an important pharmaceutical target (Smrcka et al., 2008).

We previously used random-peptide phage display screening to identify a series of peptides that bind to a "hot spot" on G$\beta\gamma$ (Scott et al., 2001). The best characterized peptide, SIGKAFKILGYPDYD (SIGK) inhibits the interaction of G$\beta\gamma$ with Gα, PLCβ2, PLCβ3, phosphoinositide 3-kinase γ and GRK2, but not with adenylyl cyclase type I or N-type calcium channels (Scott et al., 2001). The X-ray cocrystal structure of G$\beta\gamma$ with SIGK (PDB code 1XHM), together with site-directed mutagenesis, has shown that the "hot spot" is composed of a set of amino acids located at the mouth of the central tunnel on the top side of the Gβ-subunit seven-bladed β-propeller (Davis et al., 2005). This region is also known to interact with Gα, PLCβ2, GRK2 and other targets of G$\beta\gamma$ (Wall et al., 1995; Lambright et al., 1996; Ford et al., 1998; Lodowski et al., 2003).

This work was supported by the National Institutes of Health National Institute of General Medical Sciences [Grant 5R01-GM081772].
Article, publication date, and citation information can be found at http://molpharm.aspetjournals.org.
doi:10.1124/mol.110.068155.

ABBREVIATIONS: PLC, phospholipase C; GRK2, G protein-coupled receptor kinase 2; SIGK, SIGKAFKILGYPDYD; PDB, Protein Data Bank; ELISA, enzyme-linked immunosorbent assay; TBS, Tris-buffered saline; BSA, bovine serum albumin; DTT, dithiothreitol; ESI, electrospray ionization; QToF, quadrupole time-of-flight; PIP_2, phosphatidylinositol-4,5-diphosphate; SIGC, SIGCAFKILGY; NSC119910, 2-(3,4,5-trihydroxy-6-oxo-6H-xanthen-9-yl)cyclohexanecarboxylic acid; HEDS, hydroxyethyl disulfide.

Pursuing the idea that small molecules binding to subsites within the "hot spot" could be more selective inhibitors of Gβγ than peptides such as SIGK, we screened a 1990-molecule diversity set from the National Cancer Institute (NCI) (Bonacci et al., 2006). The initial screening yielded nine compounds that inhibited the binding of a phage displaying SIGK to Gβγ in an enzyme-linked immunosorbent assay (ELISA) with affinities starting at 100 nM. One of the most potent and effective compounds was selenocystamine. In this study, we investigated the mechanism of action of selenocystamine and found that selenocysteamine (half selenocystamine) forms a covalent complex with Gβγ by a reversible redox mechanism. We developed a strategy to selectively target redox reversible compounds to a specific site on Gβγ by using structural information about the "hot spot."

Materials and Methods

Competition ELISA. One microgram of streptavidin in 40 μl of TBS was immobilized in each well of a 96-well plate by incubation overnight at 4°C. Each well was blocked with 100 μl of 2% bovine serum albumin (BSA) in TBS by incubation for 1 h at 4°C, followed by three washes with TBS plus 0.5% Tween 20. Forty microliters of 25 nM biotinylated $G\beta_1\gamma_2$ ($bG\beta_1\gamma_2$), with biotin incorporated via an N-terminal acceptor peptide on $G\beta_1$, were added to each well and incubated for 1.5 h at 4°C. After three washes with TBS plus 0.5% Tween 20, small molecules/peptides and 10^9 SIGK-displaying phage particles were added simultaneously and incubated for 1 h at 4°C. The wells were then washed six times with TBS plus 0.5% Tween 20. Forty microliters of a 1:5000 dilution of horseradish peroxidase-conjugated anti-M13 antibody (GE Healthcare, Chalfont St. Giles, Buckinghamshire, UK) were subsequently added to each well and incubated for 1 h at room temperature. The wells were then washed six times with TBS plus 0.5% Tween 20, and 40 μl of 2,2′-azino-bis(3-

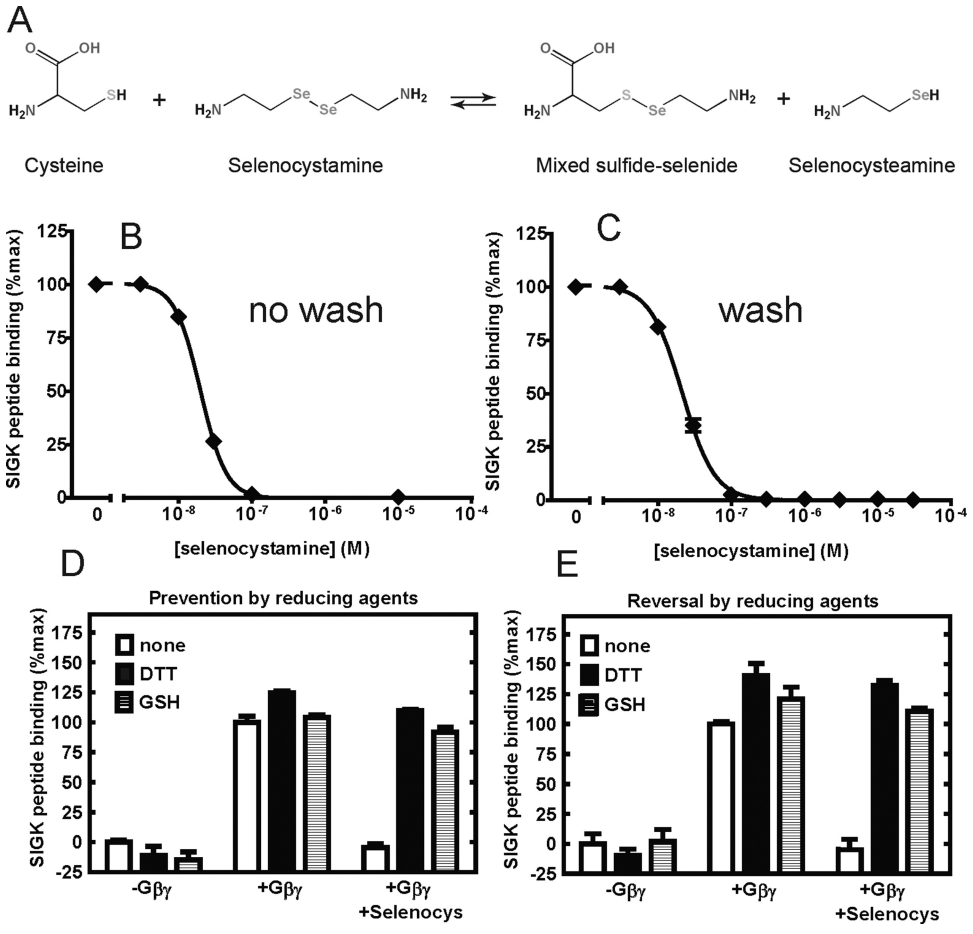

Fig. 1. A, reaction of selenocystamine with cysteine. Selenocystamine is known to react with protein cysteines to form mixed sulfide-selenides and selenocysteamine. B, titration of selenocystamine in the ELISA leaving the compound in the reaction. The experiment was carried out as described under *Materials and Methods*, Competition ELISA, except that 5×10^9 SIGK-displaying phage particles per well were used instead of 0.1×10^{10}. Data are representative of five independent experiments, shown as mean ± S.E.M. of duplicate determinations, and are fit with a sigmoid dose-response curve using the Prism 5 software (GraphPad Software, San Diego, CA). C, titration of selenocystamine in the ELISA, removing the compound from the reaction after pretreating Gβγ with it for 30 min at 4°C. The experiment was carried out as described under *Materials and Methods*. Deactivation ELISA. Data are representative of five independent experiments, shown as mean ± S.E.M. of duplicate determinations, and are fit with a sigmoid dose-response curve using the GraphPad Prism 5 software. D, prevention of the action of selenocystamine by DTT and GSH. The experiment was carried out as described under *Deactivation ELISA* in *Materials and Methods*. Biotinylated-$G\beta_1\gamma_2$ was immobilized in the wells. Five millimolar DTT or GSH (final concentration) was added together with 1 μM selenocystamine and incubated for 30 min at 4°C. The wells were washed six times with TBS plus 0.5% Tween 20, and then phage was added. Data are representative of five independent experiments and are shown as mean ± S.E.M. of duplicate determinations. E, reversal of the effect of selenocystamine by DTT and GSH. The experiment was carried out as described under *Deactivation ELISA* in *Materials and Methods*. Biotinylated-$G\beta_1\gamma_2$ was pretreated with 1 μM selenocystamine for 30 min at 4°C and then immobilized in the wells. After six washes with TBS plus 0.5% Tween 20, 5 mM DTT or GSH (final concentration) was added and incubated for 1 h at 4°C. Data are representative of five independent experiments and are shown as mean ± S.E.M. of duplicate determinations.

ethylbenzothiazoline-6-sulfonic acid) (Sigma-Aldrich, St. Louis, MO) solution were added to each of them. The colorimetric reaction was monitored at 405 nm. Nonspecific binding was subtracted for each reading and the results expressed as percentage of phage binding to $G\beta_1\gamma_2$ in controls with H_2O/dimethyl sulfoxide (depending on which solvent the small molecules/peptides were dissolved in).

Deactivation ELISA. Deactivation of $G\beta_1\gamma_2$ by redox agents was assessed as described above for the competition ELISA, except that small molecules/peptides were added and incubated for 30 min at 4°C, washed six times with TBS plus 0.5% Tween 20, followed by addition of 5×10^9 SIGK-displaying phage particles and incubation for 1 h at 4°C. Prevention of the action of the redox agents by dithiothreitol (DTT) or GSH was assessed by inclusion of 5 mM DTT or GSH (final concentration) with the small molecules. To test for reversal of the effect of the redox agents by DTT or GSH, biotinylated $G\beta_1\gamma_2$ was incubated with the small molecules/peptides for 30 min at 4°C. After six washes with TBS plus 0.5% Tween 20, 5 mM DTT or GSH (final concentration) was added and incubated for 1 h at 4°C. The wells were washed six times with TBS plus 0.5% Tween 20, and then 5×10^9 SIGK-displaying phage particles were added and incubated for 1 h at 4°C.

Analysis with Mass Spectrometry. To determine the nature of the modification produced by selenocystamine on $G\beta\gamma$, 2.5 μM $G\beta_1$6hisγ_2C68S in 20 mM ammonium acetate, pH 7.0, was incubated with 20 μM selenocystamine for 15 min and analyzed in a nano ESI QToF mass spectrometer (Synapt; Waters, Milford, MA) with sampling cone and extraction cone voltages at 80 and 2.5 V, respectively. To maintain intact $G\beta\gamma$ complexes, the collision cell voltage was set at 10 V. The collision cell voltage was increased to 80 V to promote collision-induced dissociation of the $G\beta$ subunit from the $G\gamma$ subunit and other noncovalent interactions without fragmentation of the peptide backbone.

$G\beta\gamma$-$G\alpha_i$ Interactions. Inhibition of the interaction between $G\beta_1\gamma_2$ and $G\alpha_i$ was measured as follows: 10 nM biotinylated-$G\beta_1\gamma_2$ was pretreated with 1 μM selenocystamine in a final volume of 200 μl of pulldown buffer (20 mM HEPES, pH 8.0, 1 mM EDTA, 1.2 mM $MgCl_2$, 150 mM NaCl, 0.1% Lubrol, and 10 μM GDP) for 30 min at 4°C and then incubated with 10 nM $G\alpha_i$ for 2 h at 4°C. Subsequently, 40 μl of prewashed streptavidin-agarose beads were added, and the reaction was incubated for 2 h at 4°C. The beads were centrifuged and washed three times with 500 μl of pulldown buffer. Twenty-five microliters of 2× SDS-polyacrylamide gel electrophoresis sample buffer were then added, followed by boiling for 10 min, separation by SDS-polyacrylamide gel electrophoresis, and transfer to nitrocellulose. Membranes were probed with a 1:2000 dilution of anti-$G\alpha_i$ antibody or 1:5000 anti-$G\beta$ (B600) antibody followed by a 1:10,000 dilution of goat anti-rabbit IRDye 800CW and scanned on an Odyssey Infrared Imaging System (LI-COR Biosciences, Lincoln, NE).

$G\beta\gamma$- GRK2 Interactions. Inhibition of the interaction between $G\beta_1\gamma_2$ and GRK2 was measured as follows: 15 μl of prewashed SPHERO streptavidin-polystyrene particles were incubated with 20 nM biotinylated-$G\beta_1\gamma_2$ in a final volume of 100 μl of flow cytometry buffer (20 mM HEPES, pH 8.0, 50 mM NaCl, 0.1% Lubrol, and 0.1% bovine serum albumin) for 1.5 h at 4°C. After washing the beads twice with 100 μl of flow cytometry buffer, the indicated concentrations of selenocystamine were added and the reactions were incubated for 30 min at 4°C. Alexa Fluor-532 (10 nM; Invitrogen, Carlsbad, CA)-labeled GRK2 was next added, and the reactions were incubated for 1 h at 4°C. The bead-associated fluorescence was then recorded in a FACSCanto flow cytometer (BD Biosciences, San Jose, CA).

PLCβ2 Activity Assay. Inhibition of the $G\beta\gamma$-dependent activation of PLCβ2 was measured as follows: phospholipid micelles containing 50 μM phosphatidylinositol-4,5-diphosphate (PIP_2), 200 μM phosphatidylethanolamine, and [^{3}H]PIP_2 (3.0×10^{-3} μCi/assay) were prepared by sonication in 50 mM HEPES, pH 7.2, 3 mM EGTA, and 80 mM KCl. After sonication, 1 mg/ml BSA and 0.1% *n*-octyl-β-D-glucopyranoside were added. Next, 200 nM $G\beta_1\gamma_2$ was added, and the reactions were incubated for 15 min on ice. The indicated concentrations of selenocystamine were then added, and the reactions were incubated for 15 min on ice. After that, 0.5 ng of PLCβ2 and 1.5 mM $CaCl_2$ were added to a final volume of 60 μl, and the reactions were incubated for 30 min at 30°C and then transferred back to the ice bath. The reactions were terminated by addition of 200 μl of 10% trichloroacetic acid, and the proteins and lipids were removed by precipitation with 100 μl of 10 mg/ml BSA and centrifugation for 5 min at 3000 rpm. Soluble [^{3}H]inositol-1,4,5-trisphosphate released in the reaction was then measured by analyzing 300 μl of supernatant by liquid scintillation counting for 5 min.

Synthesis of SIGC(-Cysteamine). SIGCAFKILGY-amide was added to a 5 mM solution of cysteamine-HCl at pH 8.0 to a final concentration of 0.5 mM in a total reaction volume of 15 ml. After overnight incubation with exposure to air, the resulting mixture was analyzed by high-performance liquid chromatography and mass spectrometry to demonstrate that stoichiometric 1:1 modification of SIGC with cysteamine occurred. The resulting mixture was acidified with trifluoroacetic acid and passed through a C18 cartridge to separate modified SIGC(-cysteamine) from free cysteamine, and the SIGC(-cysteamine) peptide was eluted with acetonitrile followed by lyophilization. Identity and purity of the SIGC(-cysteamine) peptide was confirmed by liquid chromatography and liquid chromatography-mass spectometry (MS).

Results

Characterization of the Modification Produced by Selenocystamine. Selenocystamine (Fig. 1A) inhibits the binding of a phage displaying SIGK to $G\beta\gamma$ in an ELISA with IC_{50} of 20 nM (Fig. 1B). Selenocystamine is known to react with cysteines to form mixed sulfide-selenides (Jacob et al., 1999), which suggests that selenocystamine could covalently modify $G\beta\gamma$ through a redox mechanism. If $G\beta\gamma$ were to be covalently modified in the presence of selenocystamine, pretreatment of $G\beta\gamma$ with selenocystamine should prevent SIGK binding even if the compound were removed from the reaction before addition of SIGK. To test this hypothesis, we pretreated $G\beta\gamma$ with selenocystamine for 1 h, followed by extensive washing before SIGK-phage addition. As shown on Fig. 1C, selenocystamine inhibited $G\beta\gamma$ with IC_{50} around 20 nM even after extensive washing, suggesting formation of a covalent complex or very tightly bound compound.

We predicted that the reducing agents DTT and GSH would prevent the action of selenocystamine by breaking the diselenide bridge before selenocystamine could react with $G\beta\gamma$. To test this prediction, we added an excess of DTT or GSH before and during incubation with selenocystamine. As shown in Fig. 1D, both DTT and GSH were able to prevent selenocystamine-dependent inhibition of $G\beta\gamma$ interactions with SIGK. We then tested whether reducing agents could reverse the selenocystamine-dependent inhibition of $G\beta\gamma$-SIGK interactions by washing away selenocystamine as described above, followed by treatment of the immobilized-modified $G\beta\gamma$ with DTT and GSH. As shown on Fig. 1E, both DTT and GSH were able to reverse the inhibitory effect of selenocystamine.

There are two cysteine residues in the vicinity but only $G\beta\gamma$C204 is directly in the SIGK binding site (Davis et al., 2005). To test whether selenocystamine blocks peptide binding by modifying $G\beta\gamma$C204, we tested SIGK-phage binding to a mutant with $G\beta$Cys204 changed to alanine ($G\beta\gamma$C204A). This mutant binds SIGK-phage but the signal is only 20% of that of wild-type $G\beta\gamma$, indicating that $G\beta$Cys204 is important

for peptide binding but not absolutely required. As shown on Fig. 2A, 1 μM selenocystamine does not inhibit binding of SIGK-phage to GβγC204A. This demonstrates that GβCys204 is required for selenocystamine-dependent inhibition of SIGK binding, suggesting that selenocystamine modifies GβγC204 in the "hot spot" to inhibit Gβγ interactions with SIGK.

The data above suggest that modification of Gβ204 is critical for inhibition of Gβγ-SIGK interaction, but there are 13 free cysteines in $G\beta_1$ and 1 free cysteine in $G\gamma_2$ that could also be modified. In addition, it is not clear what type of oxidative modification is occurring upon selenocystamine treatment. To determine the nature of the modification of Gβγ by selenocystamine and the number of sites modified by selenocystamine, $G\beta_1\gamma_2$ was treated with excess selenocystamine (20 μM) for 30 min followed by analysis by intact

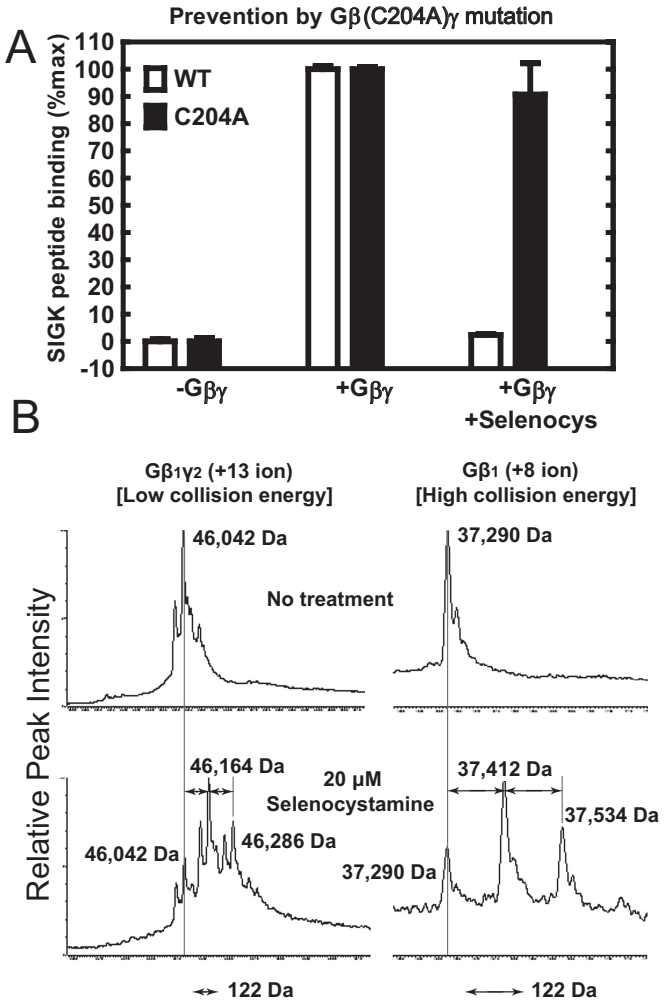

Fig. 2. A, action of selenocystamine on the GβC204A-mutant Gβγ. The experiment was carried out as described *Deactivation ELISA* in *Materials and Methods*. Biotinylated-$G\beta_1$(C204A)γ_2 was pretreated with 1 μM selenocystamine for 30 min at 4°C, and then immobilized in the wells. After six washes with TBS plus 0.5% Tween 20, 5×10^9 SIGK-displaying phage particles were added per well. Data are representative of five independent experiments and are shown as mean ± S.E.M. of duplicate determinations. B, mass spectrum of selenocystamine-treated Gβγ. Top left, $G\beta_1$6hisγ_2C68S (2.5 μM) in 20 mM ammonium acetate, pH 7.0, was analyzed in a Waters "Synapt" nano ESI QToF Mass Spectrometer. +12, +13, and +14 charged species were observed. Only the +13 charged species is shown for simplicity. The major peak at 3542.66 (46,042 Da) represents the Gβγ heterodimer where Gβ has the N terminal Met cleaved and Gγ subunits that have not been processed. Other peaks represent either differential N terminal processing of Gγ or ion adducts. Bottom left, $G\beta_1$6hisγ_2C68S (2.5 μM) in 20 mM ammonium acetate, pH 7.0, was incubated with 20 μM selenocystamine for 15 min and then analyzed as described above. Right, tandem MS dissociation of Gβ and Gγ by increasing the collision cell voltage results in release of free Gγ, whose mass is unchanged by selenocystamine (not shown), and free $G\beta_1$ (+8 ion shown for simplicity). (It is highly unlikely that a noncovalent complex between selenocystamine and Gβ survive these collision conditions necessary to dissociate Gβ from Gγ.)

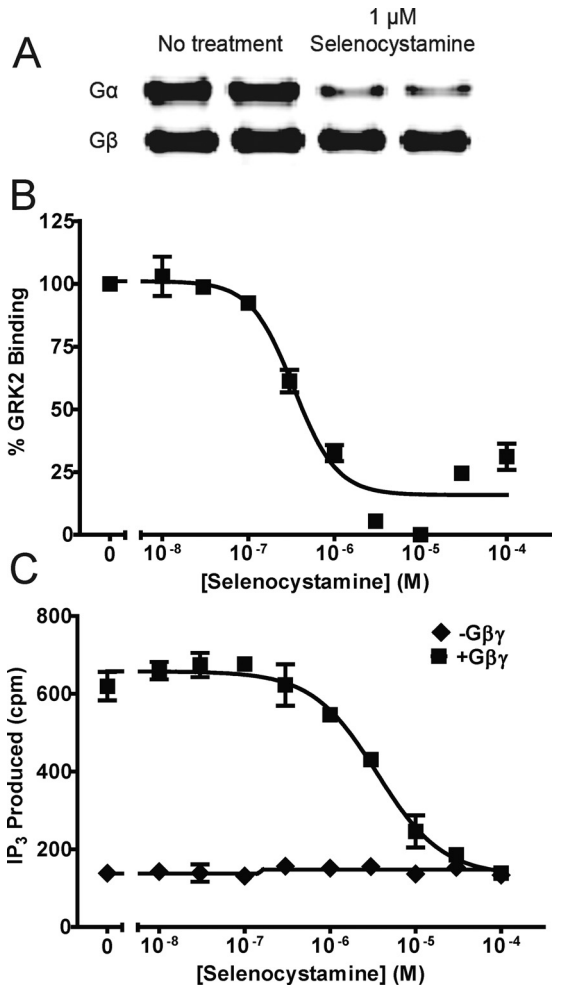

Fig. 3. Effect of selenocystamine on the interaction between Gβγ and three physiological binding partners. A, pull-down assay against $G\alpha_i$. Ten nanomolar biotinylated-$G\beta_1\gamma_2$ was pretreated with 1 μM selenocystamine, then incubated with 10 nM $G\alpha_i$, and finally immobilized on streptavidin-agarose beads. Associated $G\alpha_i$ was detected with antibody to $G\alpha_i$, and Gβγ was detected with antibody specific to the C terminus of Gβ (B600). Data are representative of two independent experiments. B, flow cytometry GRK2 binding assay. 20 nM biotinylated-$G\beta_1\gamma_2$ was immobilized on streptavidin-polystyrene particles, treated with selenocystamine at the shown concentrations, and finally incubated with 10 nM Alexa Fluor-532-labeled GRK2. The bead-associated fluorescence was recorded in a BD FACSCanto flow cytometer. Data are representative of two independent experiments, are corrected for background, are shown as mean ± S.E.M. of duplicate determinations, and are fit with a sigmoid dose-response curve using the Prism 5 software. C, PLCβ2 activity assay. Purified PLCβ2 (0.5 ng) was assayed with 1.5 mM $CaCl_2$ and selenocystamine at the shown concentrations, in the presence or absence of 200 nM purified $G\beta_1\gamma_2$. The reactions were incubated for 30 min at 30°C. [^{3}H]inositol-1,4,5-trisphosphate released from sonicated phospholipid micelles containing 50 μM PIP_2, 200 μM phosphatidylethanolamine, and [^{3}H]PIP_2 (3.0×10^{-3} μCi/assay) was measured by liquid scintillation counting. Data are representative of two independent experiments, are shown as mean ± S.E.M. of duplicate determinations, and are fit with a sigmoid dose-response curve using the Graph Pad Prism 5 software.

protein mass spectrometry. This technique measures the mass of assembled, intact, noncovalent protein complexes and has an advantage over tryptic peptide MS in that it allows assessment of the total number of modifications that occur on the protein. We observed ions corresponding to the +12, +13, and +14 charged species of Gβγ but only the +13 ion is shown for simplicity in Fig. 2B, left. Figure 2B, top left, shows untreated Gβγ and the peak at 3542.67 (46,042 Da) represents the Gβγ heterodimer with the β subunit N-terminally processed and acetylated and 6Hisγ_2(C68S) unprocessed. The other peaks in the spectrum represent complexes with variously processed Gγ species with various degrees of N-terminal methionine cleavage, N-terminal acetylation, or adduct formation. After treatment with selenocystamine (Fig. 2B, bottom left) the peak at 3542 is diminished with appearance of a new peak at 3552.06 (46,164 Da), corresponding to a mass increment of 122 Da (equal to one-half the molecular weight of selenocystamine minus 1 [the proton lost by the cysteine]) and representing Gβγ with one molecule of selenocysteamine attached. A second peak appears at 3561.43 (46,286 Da), corresponding to a mass increment of 244 Da and representing Gβγ with two molecules of selenocysteamine attached. Thus, treatment with selenocystamine resulted in attachment of a selenocysteamine at two positions on Gβγ with a single modification being the predominant species.

To determine on which subunit the modifications occurred, and whether they were covalent, we increased the collision cell voltage to dissociate the $G\beta_1$- and the $G\gamma_2$-subunits and any noncovalently bound molecules. Figure 2B, top right, shows the $G\beta_1$-subunit +8 ion in the untreated sample. In the selenocystamine-treated sample, new peaks representing, the $G\beta_1$-subunit with one and two molecules of selenocysteamine attached appeared (Fig. 2B bottom right). The mass of the $G\gamma_2$-subunit remained unchanged (not shown). A noncovalent complex between selenocystamine and the Gβ-subunit would be unlikely to survive the collision conditions necessary to dissociate the Gβ-subunit from the Gγ-subunit, indicating that the modifications produced by selenocystamine on the β-subunit were covalent. The ELISA with GβγC204A suggests that one of these modifications occurs on GβCys204.

Half-selenocystamine (123 Da, 10 atoms) is much smaller than SIGK, and approximately one third the size of 2-(3,4,5-trihydroxy-6-oxo-6*H*-xanthen-9-yl)cyclohexanecarboxylic acid (NSC119910; M119) (370 Da, 45 atoms), which is one of the most potent noncovalent inhibitors of Gβγ (Bonacci et al., 2006). To determine whether this small modification disrupts interactions between Gβγ and physiological binding partners, we tested the ability of selenocystamine to inhibit interactions of Gβγ with $G\alpha_{i1}$, GRK2, and PLCβ2 (Fig. 3, A–C). Selenocystamine inhibited Gβγ protein-protein interactions with these targets in all cases, with IC_{50} values of 300 nM for GRK2 and 3 μM for PLCβ2 (Fig. 3, A–C).

Determination of the Requirements Necessary to Achieve Selectivity for Gβγ and Specificity for GβCys204. Diselenides such as selenocystamine are known to react with the cysteines of many proteins (Jacob et al., 1999), yet the potency of selenocystamine in our assays (IC_{50}, 20 nM) was surprising. As a first step in determining whether the reaction with GβCys204 was driven by reactivity of the diselenide group or if there were additional Gβγ binding components, we analyzed a series of related compounds in a structure activity analysis. In a pure bimolecular reaction, the reaction rate and the equilibrium constant heavily depend on the pK_a of the leaving thiol or selenol; the lower the pK_a of the thiol (or selenol), the higher the reactivity and the lower the IC_{50} of the disulfide (or diselenide). First we tested cystamine (Table 1), the less reactive sulfur analog of selenocystamine. Cystamine is also known to react with cysteines, but in this case, to form mixed disulfides (Gilbert, 1990). The pK_a of selenocysteamine is 5.50 (Arnold et al., 1986), whereas the pK_a of cysteamine is 8.60 (Mezyk, 1995). Cystamine indeed inhibited Gβγ in the ELISA, but with an IC_{50} of approximately 100 μM (5000 times that of selenocystamine) (Fig. 4A). The inhibition was prevented by DTT and GSH (Fig. 4B) and reversed by DTT, but unlike the effect of selenocystamine, it was not reversed by GSH (Fig. 4C). Cystamine produced 100% inhibition at 10 mM against wild-type Gβγ, but very little inhibition at the same concentration against GβγC204A (Fig. 4D). In this case, the large difference between the IC_{50} values of selenocystamine and cystamine observed in the ELISA is probably due to their differences in pK_a.

The reaction rate and the equilibrium constant could also depend on the ability of selenocystamine or cystamine to establish specific binding interactions with Gβγ. The cocrystal structures of Gβγ with SIGK (PDB code 1XHM) (Davis et

TABLE 1
Structure-activity analysis of disulfides

Disulfide	Structure	Net Charge at pH 7.5	pK_a of Thiol	ELISA IC_{50}
Selenocystamine	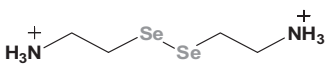	Positive	5.50[a]	20 nM
Cystamine	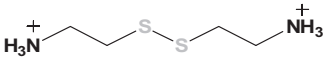	Positive	8.60[b]	100 μM
L-Cystine	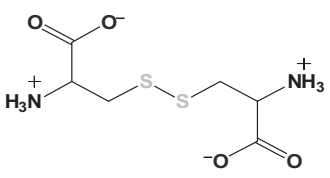	Neutral	8.33[b]	1 mM
HEDS	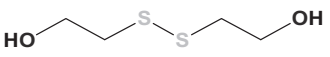	Neutral	9.50[b]	100 mM

[a] Arnold et al., 1986.
[b] Mezyk, 1995.

al., 2005) (Fig. 5A), with $G\alpha_{i1}$ (PDB code 1GOT) (Lambright et al., 1996), and with GRK2 (PDB code 1OMW) (Lodowski et al., 2003) reveal that each of these molecules has a lysine on which the ε-amino group interacts with a negative pocket in the "hot spot" of Gβγ composed of Asp228, Asn230, and Asp246 (Fig. 5B). PLCβ2 also contains a sequence similar to SIGK, ELKAYDLLSK (which also binds to Gβγ as an isolated peptide) (Sankaran et al., 1998), the first lysine of which may also interact with the negative pocket. GβCys204 is located near the negative pocket on Gβ. Given the similarity between the ε-amine on the lysine side chain and the amine of the cystamine and selenocystamine molecules, we hypothesized that the positively charged amino group of cystamine bound to the negative pocket before, during, and after cystamine/selenocystamine reacts with GβCys204.

To verify whether the positive charge of the amino group was important for the reactivity of cystamine, we tested L-cystine and hydroxyethyl disulfide (HEDS) in the ELISA (Table 1 and Fig. 4A). L-Cystine, with a net neutral charge, because of a carboxyl group in addition to each amine of cystamine, inhibited Gβγ with IC_{50} of 1 mM, 10 times that of cystamine, even though the pK_a of L-cysteine is 8.33 (Mezyk, 1995), a little lower than that of cysteamine. HEDS, also having a net neutral charge with a hydroxyl group in the place of amine of cystamine/selenocystamine, inhibited Gβγ with an IC_{50} of 137 mM, more than 1000 times that of cystamine. Given that the pK_a of the leaving group, 2-mercaptoethanol, is 9.50 (Mezyk, 1995), just 0.90 above that of cysteamine, we conclude that the loss of the positive charge is responsible for most of the loss of reactivity. Although steric effects of the carboxyl group, in addition to the charge, might explain the lesser activity of L-cystine, this cannot be the case with HEDS.

These results indicate that a positive charge, although increasing the pK_a of the leaving group and decreasing the general reactivity of the disulfide, increases the affinity for Gβγ. We have not tested any positively charged groups aside from the primary amine of selenocystamine and cystamine, but it is theoretically possible that more complex positively charged groups could establish additional specific interactions with the residues bordering Cys204 and the negative pocket, in this way increasing the affinity of the disulfide for Gβγ.

Development of the SIGC(-Cysteamine) Peptide. The results above suggest that binding directly to specific sites on Gβγ could direct the reactivity of these sulfhydryl-reactive modifiers to specific sites and possibly increase potency. On the basis of this idea, we postulated that a molecule that bound noncovalently to Gβγ could potentially deliver a reactive compound specifically to GβCys204 if it could place the

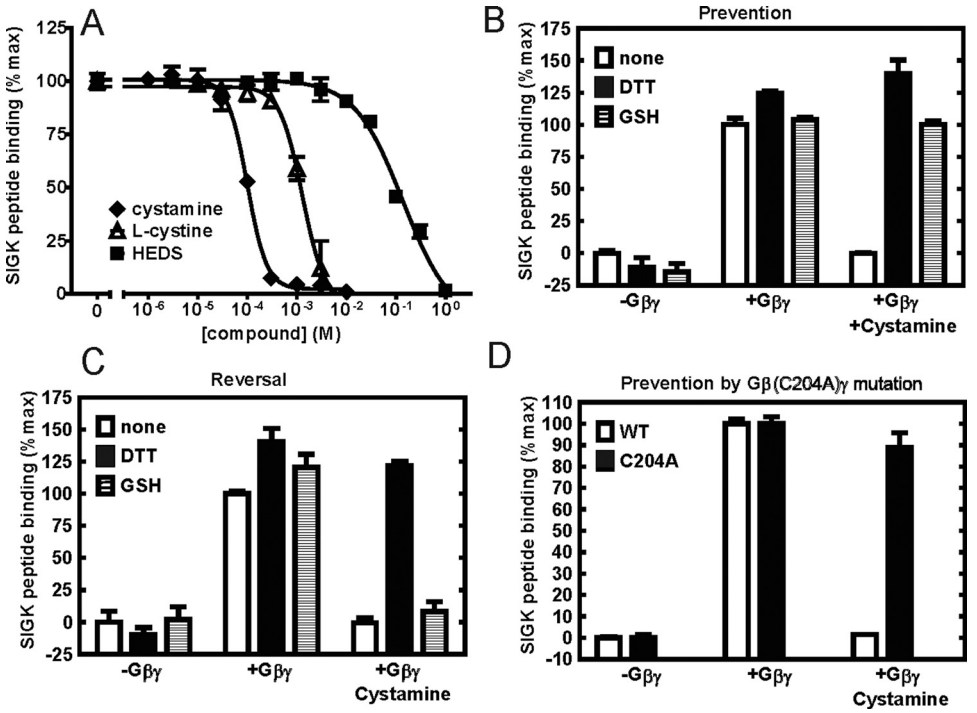

Fig. 4. A, titrations of cystamine, L-cystine, and HEDS in the ELISA. Titrations were carried out as described under *Deactivation ELISA* in *Materials and Methods*. The compounds were removed from the reaction after pretreating Gβγ with them for 30 min at 4°C. Data are representative of three independent experiments, are shown as mean ± S.E.M. of duplicate determinations, and are fit with a sigmoid dose-response curve using Prism 5 software. B, prevention of the action of cystamine by DTT and GSH. The ELISA was carried out as described under *Deactivation ELISA* in *Materials and Methods*. Biotinylated-$G\beta_1\gamma_2$ was immobilized in the wells. Five millimolar DTT or GSH (final concentration) was added together with 1 mM cystamine and incubated for 30 min at 4°C. The wells were next washed six times with TBS plus 0.5% Tween 20, and then the phage was added. Data are representative of three independent experiments and are shown as mean ± S.E.M. of duplicate determinations. C, reversal of the effect of cystamine by DTT and GSH. The ELISA was carried out as described under *Deactivation ELISA* in *Materials and Methods*. Biotinylated-$G\beta_1\gamma_2$ was pretreated with 1 mM cystamine for 30 min at 4°C, and then immobilized in the wells. After six washes with TBS plus 0.5% Tween 20, 5 mM DTT or GSH (final concentration) was added and incubated for 1 h at 4°C. Data are representative of three independent experiments and are shown as mean ± S.E.M. of duplicate determinations. D, action of cystamine on the GβC204A-mutant Gβγ. The ELISA was carried out as described under *Deactivation ELISA* in *Materials and Methods*. Biotinylated-$G\beta_1\gamma_2$ was pretreated with 10 mM cystamine for 30 min at 4°C, and then immobilized in the wells. After six washes with TBS plus 0.5% Tween 20, 5×10^9 SIGK-displaying phage particles were added per well. Data are representative of five independent experiments and are shown as mean ± S.E.M. of duplicate determinations.

reactive moiety in a position to attack the thiol of GβCys204. We tested this idea by creating a modified version of SIGK. For these experiments, we used SIGKAFKILGY, a short version of SIGK that we had previously determined binds to Gβγ with an affinity similar to that of full-length SIGK. In the crystal structure of SIGK bound to Gβγ, the SIGK-Lys4 residue is very close to GβCys204. We replaced the SIGK-Lys4 residue with a cysteine and reacted this peptide (SIGC) with cysteamine to generate SIGC(-cysteamine) Fig. 5 C. After reaction of cysteamine with SIGC-C4, the functional group at C4 becomes a primary amine derived from cystamine and is connected to the peptide backbone by a linear aliphatic chain, but now the position analogous to the γ-carbon of SIGK-Lys4 aliphatic side chain is replaced by a reactive disulfide bond in SIGC(-cysteamine). This increases the length of the side chain relative to the Lys4 position of SIGK by the length of one sulfur atom and probably alters bond angles in the chain but otherwise closely mimics the lysine that it replaced. Close examination of the structure of the Gβγ-SIGK complex shows that the γ-carbon of SIGK lysine 4 is 3.5 Å from the sulfur of GβCys204. Thus, the disulfide substitution at the position analogous to the SIGK-Lys4 γ carbon places the disulfide very near the reactive sulfhydryl of Cys204 but maintains the interaction of the lysine-like side chain with Gβγ.

We tested SIGC(-cysteamine) in the competition ELISA to confirm the ability to bind to Gβγ and compete for SIGK binding. SIGC(cysteamine) competes for SIGK-phage binding with an IC_{50} 100 times more potent than that of cystamine (Fig. 6A, left). Unlike the reversible binding of SIGK, inhibition of SIGK binding by SIGC(-cysteamine) persisted after washing to remove reversibly bound peptide from the reaction (Fig. 6A, right). Inhibition by SIGC(-cysteamine) was prevented by both DTT and GSH (Fig. 6B) and reversed by DTT addition after treatment of Gβγ (Fig. 6C). SIGC without cystamine modification only weakly inhibited SIGK binding indicating that a positive charge at the 4 position of the peptide is essential for inhibition.

We anticipated that SIGC(-cysteamine), unlike selenocystamine, would modify Gβγ at a single position, GβCys204, but were unsure of which half of the disulfide (cystamine, SIGC, or a mixture) would attach covalently to Gβγ. To answer these questions, we pretreated wild-type Gβγ with SIGC(-cysteamine) and analyzed it by mass spectrometry. Figure 7A, left, shows the Gβγ +13 ion (low collision energy). The peak at 3542.82 (46,044 Da) representing unreacted Gβγ (Fig. 7A, top left) disappeared upon treatment with SIGC (-cysteamine), whereas a single new peak at 3548.63 (46,119 Da), corresponding to a mass increment of 75 Da (equal to one half the molecular weight of cystamine minus 1) and representing Gβγ with a molecule of cysteamine attached, appeared (Fig. 7A, bottom left). Figure 7A, right, shows the free β-subunit +8 ion, released at high collision energy. The peak at 4662.24 (37,290 Da) representing the unreacted β-subunit was nearly abolished by SIGC(-cysteamine) treatment, whereas a single new peak at 4671.63 (37,365 Da), corresponding to a mass increment of 75 Da and representing the β-subunit with a molecule of cysteamine attached, appeared (Fig. 7A, bottom right). No peaks were detected corresponding to $Gβ_1$ or $Gγ_2$ with SIGC attached. Thus, SIGC(-cysteamine) efficiently transferred only cysteamine to a single position in the β-subunit.

To confirm that the single position was Cys204, we tested SIGC(-cysteamine) in the ELISA against GβC204A. As shown in Fig. 7B, SIGC(-cysteamine) competitively inhibited binding of SIGK-phage to GβC204A in manner that was reversed by washing, indicating that the protein GβC204A could not be covalently modified by SIGC(-cysteamine). Thus, SIGC(-cysteamine) efficiently and specifically delivers cys-

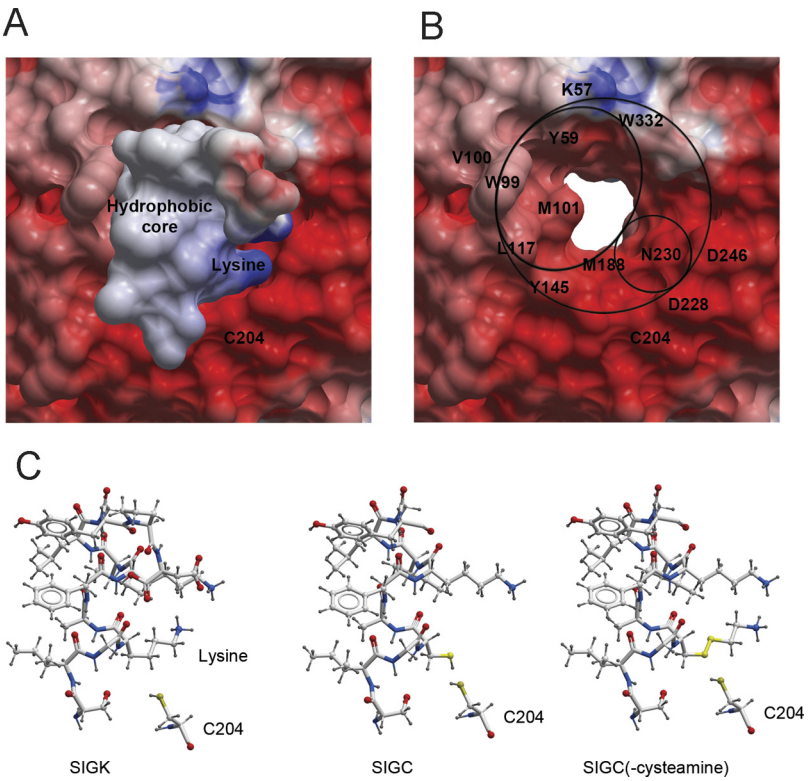

Fig. 5. A, SIGK bound to the Gβγ "hot spot." Electrostatic surface representation prepared with the Molsoft ICM-Pro software from Davis et al., 2005 (PDB code 1XHM). Positively charged areas are in blue, negatively charged in red, and hydrophobic in white. The hydrophobic core in SIGK interacts with a hydrophobic pocket in the Gβγ "hot spot," whereas Lys4 interacts with a negative pocket. B, Gβγ "hot spot" without SIGK bound to it. Electrostatic surface representation of the Gβγ "hot spot" (large circle) without SIGK bound. Trp332, Lys57, Tyr59, Trp99, Val100, Met101, Leu117, Tyr145, and Met188 comprise a hydrophobic pocket (oval) that interacts with the hydrophobic core of SIGK. Asp228, Asn230, and Asp246 delimit a negative pocket (small circle) that interacts with the first lysine of SIGK. C, SIGK, SIGC, and SIGC(-cysteamine). Stick and ball representations prepared with the Molsoft ICM-Browser software from the structure published by Davis et al., 2005 (PDB code 1XHM). When SIGK is bound to Gβγ, the side chain of Lys4 is near Cys204.

teamine to covalently modify Cys204 in the Gβγ "hot spot" leading to inhibition of protein-protein interactions.

Discussion

We used a series of high-throughput technologies to identify peptides and small molecules that bind to a "hot spot" on Gβγ (Scott et al., 2001; Bonacci et al., 2006). In the course of analyzing these small molecules, we found that a class of these compounds acts by reversible redox modification of Gβγ (A. L. Dessal and A. V. Smrcka, unpublished data). In this study, we moved from discovery of a susceptible cysteine on the β-subunit, which can be modified by relatively nonselective compounds acting in a redox manner, to the design of a selective peptide that specifically and efficiently transfers a cysteamine moiety to GβCys204. This could establish the basis for the design of selective small-molecule irreversible inhibitors and covalent modifiers of Gβγ.

Selenocystamine, cystamine, SIGC(-cysteamine), and the other molecules that covalently modify Cys204 produced 100% inhibition in the ELISA in conditions under which our most potent noncovalent binders [such as M119 or gallein (3′,4′,5′,6′-tetrahydroxyspiro[isobenzofuran-1(3*H*),9′-(9H) xanthen]-3-one)] could not achieve more than 75%. This means that covalent modifiers of Gβγ might be not only more potent but also more efficacious pharmacological agents than the noncovalent binders. The effect of covalent modifiers might also last longer than that of the noncovalent binders, especially when they produce modifications that cannot be reversed by GSH, as in the case of the addition of a cysteamine moiety.

Selenocystamine disrupted the interaction of Gβγ with the three cellular binding partners that were tested: $G\alpha_{i1}$, GRK2, and PLCβ2. Inhibition of the interaction between Gβγ and effectors is a potential site for pharmacological interventions (Koch et al., 1995; Iaccarino and Koch, 2003; Li et al., 2003). We identified a number of small molecules that bind to the "hot spot." We have tested two of these molecules, gallein and the related molecule M119, in a number of in vivo models of disease (Lehmann et al., 2008; Mathews et al., 2008; Casey et al., 2010). M11 enhances the potency of morphine-dependent analgesia, whereas gallein was very effective at inhibiting inflammation in a foot-pad inflammation assay. Molecules that bind to the "hot spot" have the potential to be useful in the treatment of heart failure. M119 and gallein are reversible inhibitors of Gβγ. A covalent modifier of Gβγ may have advantages in terms of duration of action but has the potential for nonspecific effects. The strategy we show here could allow for the development of covalent modifiers with increased specificity for Gβγ.

Although the modification produced by SIGC(-cysteamine) resisted reversal by GSH in the ELISA, the initial modification of Gβγ was prevented by GSH. It remains to be seen

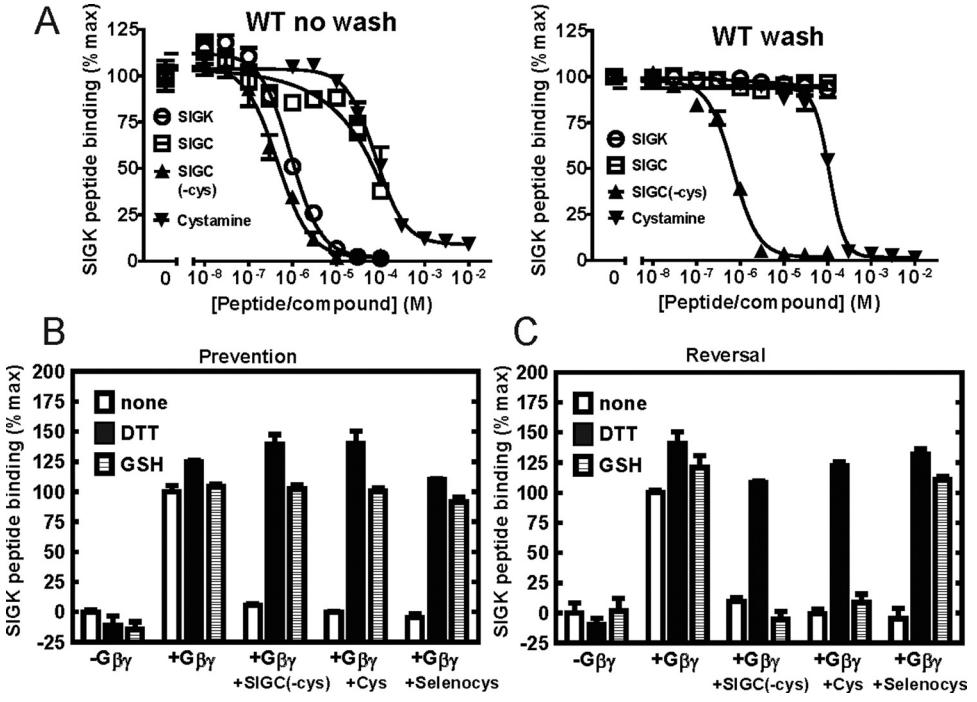

Fig. 6. A, titration of SIGC(-cysteamine) in the ELISA. Left, titration of SIGC(-cysteamine) in the ELISA leaving the peptide in the reaction. The experiment was carried out as described under *Deactivation ELISA* in *Materials and Methods*, except that 5×10^9 SIGK-displaying phage particles per well were used instead of 10^9. Right, titration of SIGC(-cysteamine) in the ELISA removing the peptide from the reaction after pretreating Gβγ with it for 30 min at 4°C, as described under *Deactivation ELISA* in *Materials and Methods*. Data are representative of two independent experiments, are shown as mean ± S.E.M. of duplicate determinations, and are fit with a sigmoid dose-response curve using GraphPad Prism 5. B, prevention of the action of SIGC(-cysteamine) by DTT and GSH. The ELISA was carried out as described under *Deactivation ELISA* in *Materials and Methods*. Biotinylated-$G\beta_1\gamma_2$ was immobilized in the wells. Five millimolar DTT or GSH (final concentration) was added together with 10 μM SIGC(-cysteamine), 1 mM cystamine, or 1 μM selenocystamine and incubated for 30 min at 4°C. The wells were next washed six times with TBS plus 0.5% Tween 20, and then the phage was added. Data are representative of two independent experiments and are shown as mean ± S.E.M. of duplicate determinations. C, reversal of the effect of SIGC(-cysteamine) by DTT and GSH. The ELISA was carried out as described under *Deactivation ELISA* in *Materials and Methods*. Biotinylated-$G\beta_1\gamma_2$ was pretreated with 10 μM SIGC(-cysteamine), 1 mM cystamine, or 1 μM selenocystamine for 30 min at 4°C, and then immobilized in the wells. After six washes with TBS plus 0.5% Tween 20, 5 mM DTT or GSH (final concentration) was added and incubated for 1 h at 4°C. Data are representative of two independent experiments and are shown as mean ± S.E.M. of duplicate determinations.

whether SIGC(-cysteamine) can resist the protective action of GSH in the cell. Nevertheless, to avoid potential problems with GSH, other (less reactive) groups might be used in place of disulfides (e.g., monofluoroalkyl ketones and acyloxymethyl ketones) (Shaw, 1990; Krantz et al., 1991; Smith et al., 2002; Vicik et al., 2006). This strategy of avoiding inactivation by GSH by using monofluoroalkyl ketones and acyloxymethyl ketones has successfully been applied in the development of cysteine protease inhibitors (Vicik et al., 2006).

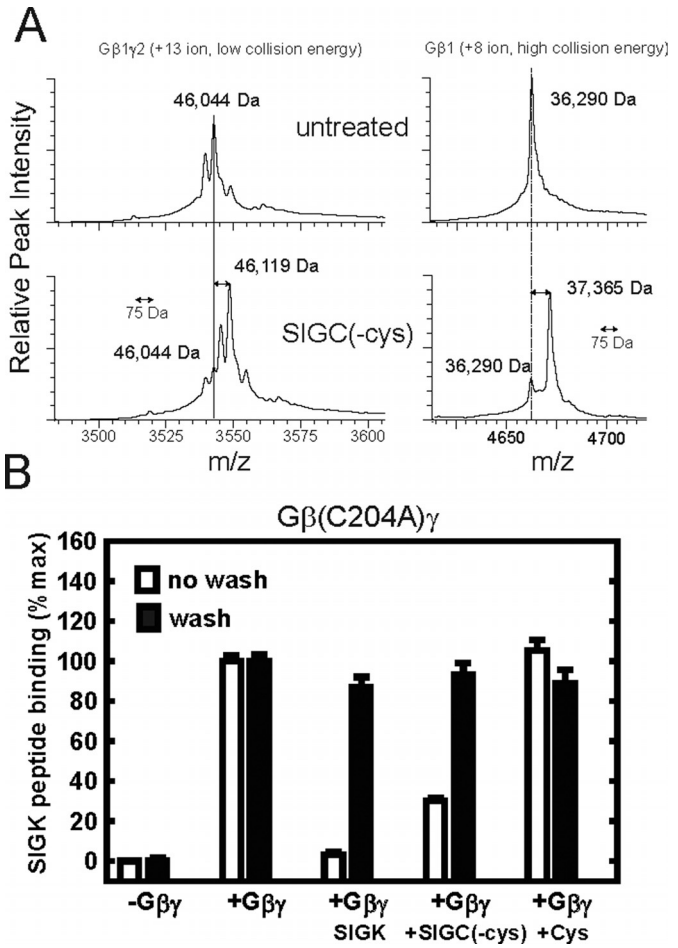

Fig. 7. A, mass spectrum of SIGC(-cysteamine)-treated Gβγ. Top left, $G\beta_1$6hisγ_2C68S (2.5 μM) in 20 mM ammonium acetate, pH 7.0, was analyzed in a Waters "Synapt" nano ESI QToF Mass Spectrometer designed for intact protein analysis. +12, +13, and +14 charged species were observed. Only the +13 charged species is shown for simplicity. Bottom left, $G\beta_1$6hisγ_2C68S (2.5 μM) in 20 mM ammonium acetate, pH 7.0, was incubated with 20 μM SIGC(-cysteamine) for 15 min and then analyzed as described above. Right, tandem MS dissociation of Gβ and Gγ by increasing the collision cell voltage results in release of free Gγ, whose mass is unchanged by SIGC(-cysteamine) (data not shown), and free $G\beta_1$ (+8 ion shown for simplicity). (It is highly unlikely that a noncovalent complex between SIGC(-cysteamine) and Gβ survive these collision conditions necessary to dissociate Gβ from Gγ.) B, action of SIGC(-cystamine) on the Gβ(C204A)γ. No wash, ELISA leaving 100 μM SIGK, 100 μM SIGC(-cysteamine), or 10 mM cystamine in the reaction. The experiment was carried out as described under *Deactivation ELISA* in *Materials and Methods*, except that 5×10^9 SIGK-displaying phage particles per well were used instead of 1×10^9. Wash, ELISA removing SIGC(-cysteamine) from the reaction after pretreating Gβγ with it for 30 min at 4°C, as described under *Deactivation ELISA* in *Materials and Methods*. Data are representative of two independent experiments and are shown as mean ± S.E.M. of duplicate determinations.

Authorship Contributions

Participated in research design: Smrcka and Dessal.
Conducted experiments: Dessal, Prades, and Smrcka.
Contributed new reagents or analytic tools: Prades and Giralt.
Performed data analysis: Dessal, Prades, and Smrcka.
Wrote or contributed to the writing of the manuscript: Dessal, Smrcka, and Giralt.
Other: Smrcka acquired funding for the research.

References

Arnold AP, Tan KS, and Rabenstein DL (1986) Nuclear magnetic resonance studies fo the solution chemistry or metal complexes. 23. Complexes of methylmercury by selenohydryl-containing amino acids and related molecules. *Inorg Chem* **25:**2433–2437.
Bonacci TM, Mathews JL, Yuan C, Lehmann DM, Malik S, Wu D, Font JL, Bidlack JM, and Smrcka AV (2006) Differential targeting of Gβγ-subunit signaling with small molecules. *Science* **312:**443–446.
Bookout AL, Finney AE, Guo R, Peppel K, Koch WJ, and Daaka Y (2003) Targeting Gβγ signaling to inhibit prostate tumor formation and growth. *J Biol Chem* **278:**37569–37573.
Casey LM, Pistner AR, Belmonte SL, Migdalovich D, Stolpnik O, Nwakanma FE, Vorobiof G, Dunaevsky O, Matavel A, Lopes CM, et al. (2010) Small molecule disruption of Gβγ signaling inhibits the progression of heart failure. *Circ Res* **107:**532–539.
Daaka Y (2004) G proteins in cancer: the prostate cancer paradigm. *Science STKE* **216:**re2.
Davis TL, Bonacci TM, Sprang SR, and Smrcka AV (2005) Structural and molecular characterization of a preferred protein interaction surface on G protein beta gamma subunits. *Biochemistry* **44:**10593–10604.
Dupré DJ, Robitaille M, Rebois RV, and Hébert TE (2009) The role of Gβγ subunits in the organization, assembly, and function of GPCR signaling complexes. *Annu Rev Pharmacol Toxicol* **49:**31–56.
Ford CE, Skiba NP, Bae H, Daaka Y, Reuveny E, Shekter LR, Rosal R, Weng G, Yang CS, Iyengar R, et al. (1998) Molecular basis for interactions of G protein βγ subunits with effectors. *Science* **280:**1271–1274.
Gilbert HF (1990) Molecular and cellular aspects of thiol-disulfide exchange. *Adv Enzymol Relat Areas Mol Biol* **63:**69–172.
Gilman AG (1987) G proteins: transducers of receptor-generated signals. *Annu Rev Biochem* **56:**615–649.
Hirsch E, Katanaev VL, Garlanda C, Azzolino O, Pirola L, Silengo L, Sozzani S, Mantovani A, Altruda F, and Wymann MP (2000) Central role for G protein-coupled phosphoinositide 3-kinase γ in inflammation. *Science* **287:**1049–1053.
Iaccarino G and Koch WJ (2003) Transgenic mice targeting the heart unveil G protein-coupled receptor kinases as therapeutic targets. *Assay Drug Dev Technol* **1:**347–355.
Jacob C, Maret W, and Vallee BL (1999) Selenium redox biochemistry of zinc-sulfur coordination sites in proteins and enzymes. *Proc Natl Acad Sci USA* **96:**1910–1914.
Koch WJ, Rockman HA, Samama P, Hamilton RA, Bond RA, Milano CA, and Lefkowitz RJ (1995) Cardiac function in mice overexpressing the β-adrenergic receptor kinase or a βARK inhibitor. *Science* **268:**1350–1353.
Krantz A, Copp LJ, Coles PJ, Smith RA, and Heard SB (1991) Peptidyl (acyloxy) methyl ketones and the quiescent affinity label concept: the departing group as a variable structural element in the design of inactivators of cysteine proteinases. *Biochemistry* **30:**4678–4687.
Lambright DG, Sondek J, Bohm A, Skiba NP, Hamm HE, and Sigler PB (1996) The 2.0 Å crystal structure of a heterotrimeric G protein. *Nature* **379:**311–319.
Lehmann DM, Seneviratne AM, and Smrcka AV (2008) Small molecule disruption of G protein βγ subunit signaling inhibits neutrophil chemotaxis and inflammation. *Mol Pharmacol* **73:**410–418.
Li Z, Jiang H, Xie W, Zhang Z, Smrcka AV, and Wu D (2000) Roles of PLC-beta2 and -beta3 and PI3Kgamma in chemoattractant-mediated signal transduction. *Science* **287:**1046–1049.
Li Z, Laugwitz KL, Pinkernell K, Pragst I, Baumgartner C, Hoffmann E, Rosport K, Münch G, Moretti A, Humrich J, et al. (2003) Effects of two Gbetagamma-binding proteins–N-terminally truncated phosducin and beta-adrenergic receptor kinase C terminus (betaARKct)–in heart failure. *Gene Ther* **10:**1354–1361.
Lodowski DT, Pitcher JA, Capel WD, Lefkowitz RJ, and Tesmer JJ (2003) Keeping G proteins at bay: a complex between G protein-coupled receptor kinase 2 and Gβγ. *Science* **300:**1256–1262.
Mathews JL, Smrcka AV, and Bidlack JM (2008) A novel Gβγ-subunit inhibitor selectively modulates mu-opioid-dependent antinociception and attenuates acute morphine-induced antinociceptive tolerance and dependence. *J Neurosci* **28:**12183–12189.
Mezyk SP (1995) Rate constant determination from the reaction of sulfhydryl species with the hydrated electron in aqueous solution. *J Phys Chem* **99:**13970–13975.
Oldham WM and Hamm HE (2006) Structural basis of function in heterotrimeric G proteins. *Q Rev Biophys* **39:**117–166.
Rockman HA, Koch WJ, and Lefkowitz RJ (2002) Seven-transmembrane-spanning receptors and heart function. *Nature* **415:**206–212.
Sankaran B, Osterhout J, Wu D, and Smrcka AV (1998) Identification of a structural element in phospholipase C β2 that interacts with G protein βγ subunits. *J Biol Chem* **273:**7148–7154.
Scott JK, Huang SF, Gangadhar BP, Samoriski GM, Clapp P, Gross RA, Taussig R, and Smrcka AV (2001) Evidence that a protein-protein interaction 'hot spot' on heterotrimeric G protein βγ subunits is used for recognition of a subclass of effectors. *EMBO J* **20:**767–776.

Shaw E (1990) Cysteinyl proteinases and their selective inactivation. *Adv Enzymol Relat Areas Mol Biol* **63:**271–347.
Smith RA, Copp LJ, Coles PJ, Pauls HW, Robinson VJ, Spencer RW, Heard SB, and Krantz A (2002) New inhibitors of cysteine proteinases. peptidyl acyloxymethyl ketones and the quiescent nucleofuge strategy. *J Am Chem Soc* **110:** 4429–4431.
Smrcka AV (2008) G protein βγ subunits: central mediators of G protein-coupled receptor signaling. *Cell Mol Life Sci* **65:**2191–2214.
Smrcka AV, Lehmann DM, and Dessal AL (2008) G protein betagamma subunits as targets for small molecule therapeutic development. *Comb Chem High Throughput Screen* **11:**382–395.
Vicik R, Busemann M, Baumann K, and Schirmeister T (2006) Inhibitors of cysteine proteases. *Curr Top Med Chem* **6:**331–353.
Wall MA, Coleman DE, Lee E, Iñiguez-Lluhi JA, Posner BA, Gilman AG, and Sprang SR (1995) The structure of the G protein heterotrimer $Gi\alpha_1\beta_1\gamma_2$. *Cell* **83:**1047–1058.

Address correspondence to: Alan V. Smrcka, Department of Pharmacology and Physiology, Department of Biochemistry and Biophysics, and the Aab Cardiovascular Research Institute, University of Rochester, School of Medicine and Dentistry, 601 Elmwood Avenue, Box 711, Rochester, NY 14642-8711. E-mail: alan_smrcka@urmc.rochester.edu